CMLS, Cell. Mol. Life Sci. 60 (2003) 2679–2691
1420-682X/03/122679-13
DOI 10.1007/s00018-003-3305-3

CMLS Cellular and Molecular Life Sciences

Research Article

Neuronal thread protein regulation and interaction with microtubule-associated proteins in SH-Sy5y neuronal cells

S. M. de la Monte[a,b,*], G. J. Chen[a], E. Rivera[a] and J. R. Wands[a]

[a] Department of Medicine, Rhode Island Hospital and Brown Medical School, 55 Claverick Street, Providence, Rhode Island 02903 (USA), Fax: +1 401 444 2939, e-mail: suzannedelamontemd@brown.edu
[b] Department of Pathology, Rhode Island Hospital and Brown Medical School, 55 Claverick Street, Providence, Rhode Island 02903 (USA)

Received 2 August 2003; received after revision 3 September 2003, accepted 23 September 2003

Abstract. In Alzheimer's disease (AD), neuronal thread protein (NTP) accumulates in cortical neurons and colocalizes with phospho-*tau*-immunoreactive cytoskeletal lesions that correlate with dementia. To generate additional information about the potential role of NTP in AD, we characterized its expression and regulation in human SH-Sy5y neuronal cells. Quantitative real-time reverse transcription-polymerase chain reactin and Western blot analysis demonstrated prominent insulin, moderate insulin-like growth factor, type 1 (IGF-1) and minimal nerve growth factor stimulation of NTP expression. In addition, NTP protein was more stable and it progressively accumulated in cells that were stimulated with insulin for 24 or 48 h. Metabolic labeling and phosphoamino acid analysis demonstrated phosphorylation of NTP on Serine residues, 30–60 min after insulin or IGF-1 stimulation, when glycogen synthase kinase 3β (GSK-3β) activity would no longer have been suppressed. Kinase inhibitor and in vitro phosphorylation studies demonstrated a role for GSK-3β in the positive regulation of NTP expression and phosphorylation. Coimmunoprecipitation studies demonstrated physical interactions between NTP and *tau* or microtubule-associated protein 1b (MAP-1b), and ubiquitin immunoreactivity in NTP immunoprecipitates. In summary, these studies showed that (i) NTP expression is regulated at the level of transcription by insulin and IGF-1 stimulation; (ii) NTP is phosphorylated by GSK-3β; (iii) NTP can physically interact with *tau* and MAP-1b and (iv) NTP-MAP complexes are ubiquitinated. The results suggest a functional role for NTP in relation to the turnover or processing of neuronal cytoskeletal proteins, attributes that may be modulated by insulin/IGF-1-mediated signaling.

Key words. Alzheimer's disease; insulin; gene expression; protein phosphorylation; glycogen synthase kinase; microtubule-associated proteins.

Neuronal thread protein (NTP) is an ~41-kD molecule that is encoded by an ~1.4-kB messenger RNA (mRNA) transcript expressed in the brain [1]. Using monoclonal antibodies generated against the recombinant protein, several smaller related molecules, including ~26-kD, ~21-kD and ~14–18-kD species were identified by Western blot analysis [2]. Previous studies demonstrated increased expression of the ~41-kD and ~21-kD NTP species in brains with AD [1, 2]. In addition, NTP was found to colocalize with phospho-*tau*-immunoreactive neuronal cytoskeletal lesions that correlate with dementia in AD [2]. Furthermore, the elevated levels of NTP immunoreactivity in cerebrospinal fluid of patients with early AD suggested that increased NTP expression may reflect a proximal abnormality in the neurodegeneration

* Corresponding author.

cascade [1, 3–6]. Although initial studies attempting to characterize neuronal thread protein were conducted with antibodies to the Reg gene [7–9], isolation of the NTP complementary DNA (cDNA) from the human brain library demonstrated NTP to be distinct from Reg, both at the mRNA and protein levels [1]. The explanation for the cross-reactivity is that the antibodies to Reg recognize a conformational epitope on NTP. However, recent unpublished studies performed in our laboratory using real-time quantitative reverse-transcribed polymerase chain reaction (RT-PCR) demonstrated Reg mRNA transcripts in both the brain and human neuronal cell lines. The current work concerns the expression and function of NTP and not the Reg gene.

Despite its extensive characterization in relation to AD [1, 2, 10–12], the function of NTP is still unknown. Previous studies demonstrated that NTP expression was higher in fetal and early postnatal developing brains than in mature brains [13], but following acute cerebral infarction, NTP expression was found to be transiently increased in the peri-infarct zone that participates in regeneration and repair [14]. In addition, with neuronal differentiation, NTP immunoreactivity translocates from the perikaryon to elongated neuronal cell processes [15], suggesting a possible role for this molecule in neuritic sprouting. Finally, we previously showed that NTP protein expression was modulated in response to insulin-stimulated signaling through the insulin receptor substrate, type 1 [16, 17].

To better understand the role of NTP in relation to AD-type neurodegeneration, it is essential that we characterize its normal regulation and function. In designing strategies for these investigations, consideration was given to the structural features of the NTP protein encoded by the cDNA that was isolated from an Alzheimer disease brain library (AD7c-NTP) [1]. In this regard, subsequence analysis predicted the presence of an insulin-insulin-like growth factor, type 1 (IGF-1) chimeric receptor domain, which may have relevance to function or regulation of the molecule [1]. In addition, the protein has 17 potential phosphorylation motifs, the majority (14 of 17) of which correspond to glycogen synthase kinase 3β (GSK-3β) sites [1]. GSK-3b is one of the major kinases responsible for *tau* phosphorylation in brains with AD [18].

Taking together the observations made in AD brains, cultured cells and experimental cerebral ischemia, with the computer-based analysis of NTP structure, we predicted NTP to be a phospho-protein that is regulated by insulin or IGF-1, and capable of physically associating with neuronal cytoskeletal proteins, particularly *tau*. To test this hypothesis, we examined growth factor modulation of NTP expression and phosphorylation, and assessed potential physical interactions between NTP and the microtubule-associated proteins, *tau* and MAP-1b.

Methods

Cell culture conditions

SH-Sy5y human neuronal cells were maintained in Dulbecco's modified Eagle's medium supplemented with 9 g/l glucose, 4 mM glutamine, 10 µM nonessential amino acid mixture and 10% heat-inactivated fetal calf serum (FCS). To study the effects of growth factor stimulation on NTP expression, subconfluent cultures were serum starved for 16 h, then fed with defined medium supplemented with insulin (50 nM), IGF-1 (25 nM), nerve growth factor (NGF; 5 nM) or nothing (negative control) for 0–60 min, or 24–96 h. However, for the 24–96-h studies, 0.5% FCS was added to the control cultures because complete growth factor deprivation for longer than 24 h causes apoptosis of SH-Sy5y cells. SH-Sy5y cells were selected for study because they are of human origin, and the cDNA sequence is known. Cells of rat origin, including PC12 and primary rat cortical neuron cultures, were not the major focus of investigation because the rat NTP cDNA has not yet been isolated. However, using one of the cross-reactive monoclonal antibodies, rat brain tissue was included in a limited Western-blotting study to demonstrate developmental changes in the levels of NTP.

Analysis of growth factor-stimulated NTP expression

NTP expression was evaluated using quantitative real-time RT-PCR assays and Western blot analysis. For the quantitative real-time RT-PCR studies, total RNA was isolated using TRIzol (Invitrogen, Carlsbad, CA) according to the manufacturer's protocol. Samples containing 2 µg RNA were reverse transcribed with the AMV First Strand cDNA synthesis kit (Roche, Basel, Switzerland) and random oligodeoxynucleotide primers. In parallel PCR amplifications, expression levels of amyloid precursor protein (APP) and nitric oxide synthase-3 (NOS-3) were measured as specificity controls since these molecules also have relevance to the pathology or pathogenesis of AD [19–21], but were not expected to be regulated

Table 1. Primers used for real-time quantitative RT-PCR amplification studies.

Primer*	Sequence (5′ → 3′)
NTP forward	GAG ATG GAG TTT TCG CTC TTG TTG
NTP reverse	TGC CTG TAA TCC CAG CCT ACT G
NOS-3 forward	CAG GAA GTA AGT GAG AGC CTG
NOS-3 reverse	TCC AGT AAC ACA GAC AGT GC
APP forward	GTT CTG CAT CTG CTC AAA G
APP reverse	TGC CAC CAC TAC CAC AAG TA
18s forward	GCC TCA CTA AAC CAT CCA ATC G
18s reverse	AAC CCG TTG AAC CCC ATT CG

* Primer sequences used for real-time quantitative RT-PCR studies. NTP, neuronal thread protein; NOS-3, nitric oxide synthase 3; APP, amyloid precursor protein; 18s, 18s ribosomal RNA.

in the same manner as NTP. PCR primer pairs were designed using MacVector 7.0 software (Accelrys, Oxford Molecular, Oxford, England). PCR amplifications were performed in 25-µl reactions containing 20 ng of RT product, 0.4 µM each of the forward and reverse primers (table 1), and SYBR Green I Master Mix (BioRad, Beverly, MA). The amplified signals were detected continuously with the BioRad iCycler iQ Multi-Color Real Time PCR Detection System (Hercules, CA). The following real-time PCR amplification protocol was used: (i) initial 10 min denaturation and enzyme activation at 95 °C; (ii) a three-segment amplification consisting of 40 cycles of 95 °C × 30 s, 60 °C × 45 s, and 72 °C for 30 s; and (iii) a cooling step to 4 °C. Cycle threshold detection was obtained using the iQ software, and the levels of mRNA expression (ng) in the original samples were determined from standard curves constructed with recombinant plasmid DNA. To obtain the recombinant plasmids, conserved regions of each cDNA containing the sequences amplified in the studies were cloned into the PCRII vector (Invitrogen, Carlsbad, CA), and verified by sequencing. Serial dilutions of a known amount of purified plasmid DNA were used in separate amplification reactions, and the equation of the regression line relating cycle threshold to copy number or ng DNA was used to calculate transcript abundance in the samples. To correct for differences in template loading, the ng ratios of NTP, APP or NOS3 to 18S were calculated, thereby providing indices of relative transcript abundance that were used to make intragroup and intergroup comparisons.

Protein expression studies

NTP immunoreactivity was detected by Western blot analysis, immunoprecipitation, metabolic labeling and immunofluorescence. For Western blot analysis, cells and tissues were homogenized in radioimmunoprecipitation assay (RIPA) buffer (50 mM Tris-HCl, pH 7.5, 1% NP-40, 0.25% Na-deoxycholate, 150 mM NaCl, 1 mM EDTA, 2 mM EGTA) containing protease [1 mM PMSF (phenylmethylsulfonyl fluoride), 0.1 mM TPCK (tosylphenylalanyl chloromethylketone), 1 µg/ml aprotinin, 1 µg/ml pepstatin A, 0.5 µg/ml leupeptin, 1 mM NaF, 1 mM $Na_4P_2O_7$] and phosphatase (2 mM Na_3VO_4) inhibitors. Protein concentrations were determined using the bicinchoninic acid (BCA) assay (Pierce, Rockford, IL). Samples containing 60 µg of protein were fractionated by sodium dodecyl sulfate, polyacrylamide gel electrophoresis (SDS-PAGE) [22]. Proteins were transferred to polyvinylidiene fluoride (PVDF) membranes, and nonspecific binding sites were adsorbed with SuperBlock-TBS (Pierce, Rockford, IL). The membranes were then incubated overnight at 4 °C with primary antibody (0.5–1 µg/ml) diluted in Tris-buffered saline (TBS; 50 mM Tris, 150 mM NaCl, pH 7.4) containing 1% bovine serum albumin and 0.05% Tween-20 (TBST-BSA). Immunoreactivity was detected using horseradish peroxidase (HRP) conjugated secondary antibody and enhanced chemiluminescence (ECL) reagents. Immunoreactivity was quantified using the Kodak Digital Science Imaging Station (NEN Life Sciences, Boston, MA).

For immunoprecipitation studies, cells were homogenized in Triton lysis buffer (50 mM Tris-HCl, pH 7.5, 10 mM EDTA, 1% Triton X-100) containing protease and phosphatase inhibitors as indicated above. Samples containing 500 µg of protein diluted to 1 mg/ml in Triton lysis buffer were precleared with Protein A sepharose, then incubated overnight at 4 °C with 1 µg/ml of primary antibody using constant rotation. Protein A sepharose was then added, and the samples were incubated for an additional 2 h at 4 °C with constant rotation. The immune complexes were washed 3 times in Triton lysis buffer using a standard protocol [22]. The immunoprecipitates were analyzed by Western blot analysis.

For subcellular fractionation studies, the cells were rinsed in ice-cold phosphate-buffered saline, suspended in 5 vol of ice-cold hypotonic buffer (0.25 M sucrose, 5 mM Tris-HCl, pH 7.2, 1 mM $MgCl_2$), Dounce homogenized (10 strokes, Type B pestle), then centrifuged at 3300 × g for 15 min at 4 °C to pellet nuclei. The resulting crude supernatant was divided into two fractions. One fraction was centrifuged at 60,000 × g for 30 min and the supernatant used as the cytosolic fraction. The resulting pellet was resuspended in buffer containing 50 mM NaCl, 10 mM Tris, pH 7.4, 2.5 mM $MgCl_2$ and 1% Triton X-100, and the soluble material was used as the membrane fraction. To the second crude supernatant fraction, Triton X-100 was added to achieve a concentration of 1%. The pellet obtained by centrifuging the sample at 12,000 × g was solubilized in buffer containing 50 mM NaCl, 10 mM Tris, pH 7.4, 2.5 mM $MgCl_2$, protease inhibitors, 0.5% sodium deoxycholate, 1% Tween 40 and 1% Triton X-100, and then centrifuged at 12,000 × g for 15 min to pellet insoluble debris. The corresponding supernatant was used as the cytoskeleton fraction [22]. Protease inhibitor cocktail (see Western protocol) was included in all buffers. Protein concentrations were measured using the BCA assay (Pierce, Rockford, IL).

Analysis of NTP phosphorylation

NTP phosphorylation was demonstrated by metabolic labeling of cultured cells with [^{32}P] orthophosphoric acid [22]. Phosphorylated NTP immunoprecipitated from cell lysates was detected by SDS-PAGE and autoradiography. Western blot analysis of the [^{32}P]-labeled immunoprecipitates was used to demonstrate that the phospho-proteins corresponded to NTP. As an additional strategy, NTP immunoprecipitated from cell lysates was subjected to Western blot analysis using monoclonal antibodies to phospho-Serine or phospho-Threonine. Immunoreactivity was detected with HRP-conjugated secondary anti-

body, ECL reagents and the Kodak Digital Science Imaging Station.

To identify the phosphorylated amino acids, the [^{32}P]-labeled, SDS-PAGE fractionated immunoprecipitates were transferred to Immobilon P membrane. The appropriate band (detected by autoradiography) was excised and subjected to acid hydrolysis, the products of which were analyzed by two-dimensional electrophoresis using the Hunter Thin Layer Peptide Mapping Electrophoresis System (C.B.S. Scientific Company, Del Mar, CA) according to the manufacturer's protocol. Phospho-amino acid standards were included in all analyses. In addition, affinity-purified recombinant NTP protein [1, 2] was used as a substrate for GSK-3β phosphorylation in the presence of [γ-^{32}P]ATP [22]. A nonrelevant kinase (Erk MAPK) was used as a negative control in parallel studies. The reaction products were analyzed by SDS-PAGE and autoradiography.

Effects of kinase modulators on NTP mRNA and protein levels

To determine the effects of different kinase modulators on NTP protein expression, cells stimulated with insulin or IGF-1 were metabolically labeled with [^{35}S]-methionine/cysteine (Dupont-NEN Express Labeling) [22]. NTP immunoprecipitates were fractionated by SDS-PAGE and detected by film autoradiography. Parallel insulin or IGF-1-stimulated cultures were treated with one of the kinase modulators listed in table 2, and analyzed by quantitative real-time RT-PCR or Western blot analysis to detect changes in NTP expression.

Source of antibodies and chemicals

Monoclonal antibodies to NTP were generated to recombinant protein [1, 2]. Recombinant human NGF and IGF-1 were purchased from Sigma-Aldrich Co (St. Louis, MO) and human insulin (Novolin R) was purchased from Nova Nordisk Pharmaceuticals (Princeton, NJ). Protein A sepharose was purchased from Amersham-Pharmacia Biotechnology (Arlington Heights, IL). Kinase inhibitors were purchased from CalBiochem (Carlsbad, CA). General chemical reagents were purchased from Sigma-Aldrich (St. Louis, MO) or CalBiochem (Carlsbad, CA).

Statistical analysis

Data depicted in the graphs represent the mean ± S.D. of results generated from three to six experiments. Intergroup comparisons were made using Student t-tests or analysis of variance (ANOVA) with Fisher least significant difference (LSD) post-hoc tests. Statistical analysis was performed using the Number Cruncher Statistical Systems (Dr Jerry L. Hintze, Kaysville, UT).

Results

NTP expression in SH-Sy5y neuronal cells and brain tissue using the N3I4 monoclonal antibody

Immunofluorescence studies of cultured SH-Sy5y cells localized NTP immunoreactivity to the periphery and along the inner surface of the plasma membrane (fig. 1 A-1). Parallel negative control studies included reactions in which the primary antibody was omitted or a nonrelevant antibody to hepatitis B virus was used instead (fig. 1 A-2). Two clusters of NTP-immunoreactive proteins with molecular masses of ~39–45 kD or ~18–21 kD were detected by Western blot analysis of SH-Sy5y cells (fig. 1 B). The same size NTP-immunoreactive proteins were detected by Western blot analysis of postmortem temporal lobe tissue from patients AD or normal aging (fig. 1 C) [1, 2], and cerebral cortex from different age rats (fig. 1 D). Corresponding with previous reports [1, 2], the levels of NTP in AD were higher than in normal aged control brains. In rat brains, the highest levels of NTP were observed on postnatal day 8 (fig. 1 D). Subcellular fractionation studies showed that the majority of NTP-immunoreactive proteins partitioned with the cytoskeletal and membrane fractions, whereas only a small portion was extracted in the cytosolic fraction (fig. 1 E).

Table 2. Compounds used to identify signaling pathways regulating NTP expression and phosphorylation.

Compound	Concentration	Target of inhibition
Butyrolacetone	680 nM	Cdk-5
Chelerythrine chloride	600 nM	protein kinase C
H89 dihydrochloride	50 nM	protein kinase A
PD98059	2 µM	MAP kinase kinase
SB202190	400 nM	p38 MAP kinase
Genestein	2.6 µM	protein tyrosine kinase
LY83583	2 µM	cyclic GMP-dependent kinase
Lithium chloride	1.3 mM	GSK-3β
Indirubin-3′-monoxime	180 nM	cyclin-dependent kinases
Indirubin-3′-monoxime, 5-iodo	10 nM	GSK-3β and Cdk-5

Chemical inhibitors used to evaluate signaling mechanisms regulating NTP expression and phosphorylation following insulin stimulation. Cdk, cyclin-dependent kinase; GSK-3β, glycogen synthase kinase-3β.

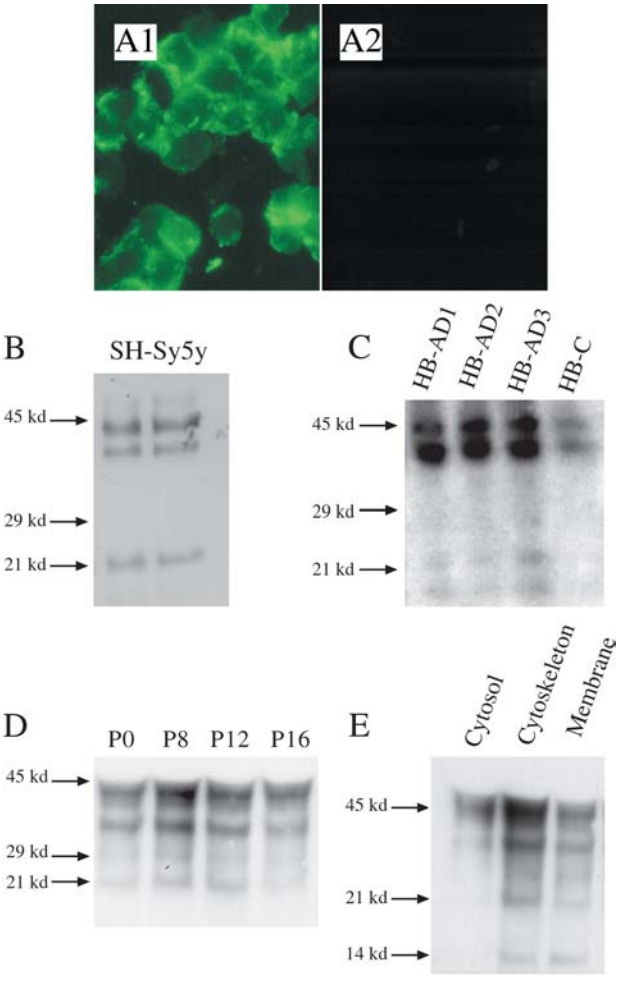

Figure 1. NTP expression in neuronal cells and brain tissue detected with the N3I4 monoclonal antibody. (*A*) Immunofluorescence detection of NTP in cultured SH-Sy5y cells. Cells were fixed, permeabilized and incubated with the cocktail of monoclonal antibodies to NTP (A1) or nonrelevant monoclonal antibody to hepatitis B surface antigen (A2). Immunoreactivity was detected using biotinylated secondary antibody and fluorescein-conjugated avidin D. Western blot analysis detection of NTP in (*B*) SH-Sy5y cells, (*C*) postmortem human temporal lobe tissue from patients with Alzheimer's disease (HB-AD1-HB-AD3) or normal aging (HB-C) and (*D*) cerebral cortex harvested from rats on postnatal day (P) 0 (birth), 8, 12 or 16. (*E*) Fractionation studies were used to demonstrate the subcellular distribution of NTP proteins in SH-Sy5y cells (see 'Methods'). NTP expression was detected using the N3I4 monoclonal antibody that was produced against the recombinant protein. Immunoreactivity was revealed with horseradish peroxidase conjugated secondary antibody, ECL reagents and digital imaging or film autoradiography Positions of the molecular weight standards are shown at the left of each panel.

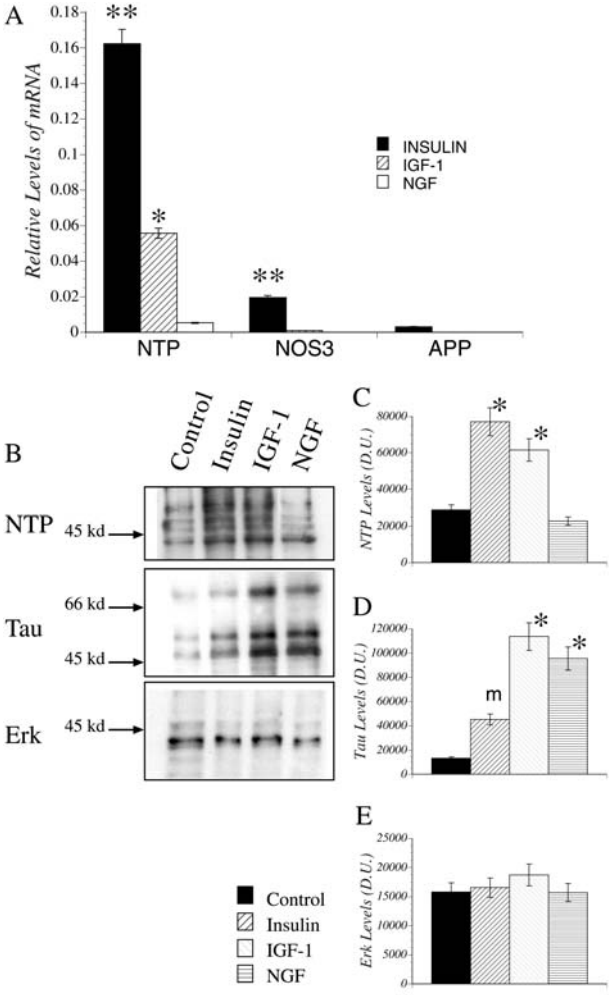

Figure 2. Growth factor modulation of NTP expression. SH-Sy5y cells were cultured in defined medium supplemented with 50 nM insulin, 25 nM IGF-1, 5 ng/ml NGF or 0.5% FCS. (*A*) NTP mRNA levels were measured using real-time quantitative RT-PCR. To evaluate the specificity of the results, mRNA levels of nitric oxide synthase 3 (NOS-3) and amyloid precursor protein (APP) were simultaneously measured. Ribosomal 18s transcripts were measured in parallel reactions to assess total RNA abundance. Primers used in the amplification reactions are listed in table 1. The nanogram quantities of mRNA or ribosomal RNA (rRNA) were calculated from standard curve equations generated with serial dilutions of purified recombinant plasmid DNA. The graph depicts calculated ratios (mean ± S.D. of NTP, NOS3 or APP mRNA to 18s transcripts measured in the same samples. (**P < 0.001 relative to IGF-1- and NGF-stimulated cells; *P < 0.001 relative to NGF-stimulated cells). (*B*) Growth factor modulation of NTP protein levels demonstrated by Western blot analysis. NTP was detected using a cocktail of monoclonal antibodies (N3I4, N2J1, N2U6) that detect additional supershifted (probably phosphorylated) bands. For comparison, growth factor-stimulated *tau* and Erk MAPK protein expression were also measured. Equivalent amounts of protein were loaded in each lane. Immunoreactivity was detected with horseradish peroxidase conjugated secondary antibody and ECL reagents. The positions of molecular weight standards are shown at the left of each panel. (*C–E*) Results of scanning digital densitometry of (*C*) NTP, (*D*) tau and (*E*) Erk MAPK protein levels from three replicate samples. Values (mean ± S.D.) posted represent arbitrary densitometry units (D.U.; *P < 0.01 relative to control).

Growth factor modulation of NTP expression

Quantitative real-time RT-PCR, Western blot analysis and metabolic labeling studies were used to examine NTP expression in relation to growth factor stimulation (fig. 2). For the quantitative RT-PCR studies, NOS3 and APP expression levels were simultaneously measured because

these genes have relevance to AD-type neurodegeneration but were not expected to be modulated in the same manner as NTP (fig. 2A). The NTP mRNA levels were highest in the insulin-stimulated intermediate in IGF-1-stimulated cells and lowest in the NGF-stimulated cells ($P < 0.001$ for intergroup differences). NOS-3 mRNA expression also increased with insulin stimulation, although the levels were substantially lower than those of NTP. In contrast, APP mRNA levels were not increased by insulin, IGF-1 or NGF stimulation, indicating that the APP gene was not transcriptionally modulated by growth factor stimulation under the experimental conditions employed.

Western blot analysis of SH-Sy5y cells cultured for 24 h in 0.5% FCS (control), insulin, IGF-1 or NGF demonstrated high levels of NTP immunoreactivity in insulin- and IGF-1-stimulated cells, and relatively low levels of NTP in control and NGF-stimulated cells (figs 2B, C). In these studies, NTP was detected using a cocktail of monoclonal antibodies (N3I4, N2J1, N2U6) to demonstrate supershifted (probably phosphorylated) forms of NTP. *Tau* protein expression was simultaneously studied and found to be modulated by growth factor stimulation; however, the highest levels of *tau* were observed in IGF-1- and NGF-stimulated cells rather than insulin-stimulated cells (figs 2B, D). As a negative control, total Erk MAPK protein levels were also assayed and found to not vary with growth factor stimulation (figs 2B, E). Corresponding with the real-time RT-PCR results, NOS-3 and APP proteins were also not substantially modulated by growth factor stimulation (data not shown).

The time course analyses of growth factor-stimulated NTP turnover/stability and expression were performed to assess the dynamics of NTP protein turnover and intracellular accumulation. Cells were serum-starved for 16 h, then stimulated with insulin or IGF-1. To examine NTP protein stability, the cells were metabolically labeled for 3 h with [^{35}S]Met/Cys, and then incubated for up to 2 h in isotope-free medium with continued growth factor stimulation. NTP was immunoprecipitated from the cell lysates, fractionated by SDS-PAGE and detected by autoradiography. The identity of the NTP molecules was confirmed by Western blot analysis of the immunoprecipitates. Radiolabeled, newly synthesized NTP molecules were found to persist longer in the insulin-compared with IGF-1-stimulated cells (fig. 3A), indicating increased stability and slower turnover with insulin stimulation.

To examine the effects of insulin stimulation on NTP protein levels over time, Western blot analysis was performed with cells that had been growth-factor deprived for 16 h, then stimulated with 50 nM insulin for 0, 6, 12, 18, 24 or 48 h. The levels of immunoreactivity were measured using digital image densitometry. After 16 h of growth factor deprivation (time 0), NTP protein expression was very low level. With increasing duration of insulin stimulation, the levels of the ~39–45-kD NTP protein progressively increased and were highest at the 48-h time point (figs 3B, C). The smaller mass NTP-immunoreactive proteins were initially detected after nearly 18 h of insulin stimulation (fig. 3B).

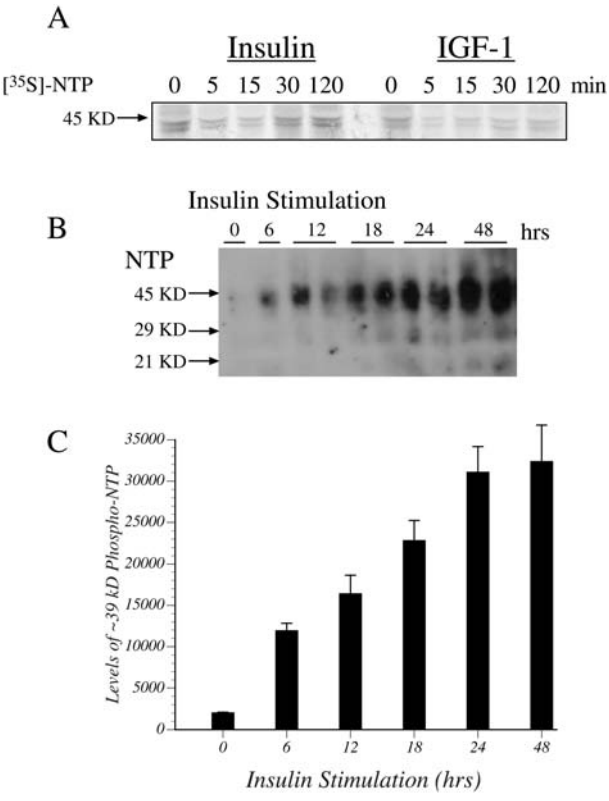

Figure 3. Time course analysis of growth factor-stimulated NTP expression and stability in SH-Sy5y cells. (*A*) Cells were stimulated with 50 nM insulin or 25 nM IGF-1. The cells were then metabolically labeled with [^{35}S]-Methionine/Cysteine for 3 h, followed by a further incubation in isotope-free defined medium for up to 2 h. [^{35}S]-labeled NTP molecules were immunoprecipitated with the N3I4 monoclonal antibody, fractionated by SDS-PAGE, transferred to PVDF membranes and detected by film autoradiography. Equivalent amounts of protein were loaded in each lane. (*B*) Insulin-stimulated NTP protein expression and accumulation. Subconfluent cultures of SH-Sy5y cells were growth factor deprived for 16 h, then stimulated with 50 nM insulin for 6, 12, 18, 24 or 48 h. Proteins extracted from the cells were evaluated by Western blot analysis using the N3I4 monoclonal antibody to NTP. Immunoreactivity was detected using horseradish peroxidase conjugated secondary antibody and ECL reagents. Equivalent amounts of protein were loaded into each lane. The positions of molecular weight standards are shown at the left of each panel. The broad bands represent unresolved doublets as shown in figures 1B–E. (*C*) Densitometric analysis of the Western blot signals shown in (*B*). The levels of immunoreactivity were measured using the Kodak Digital Science Imaging Station, and the values posted (mean ± S.D.) represent arbitrary densitometry units (D.U.).

Signaling pathways regulating NTP expression

To determine potential mechanisms by which insulin regulates NTP expression, SH-Sy5y cells were pretreated for 2 h with one of the kinase modulators listed in table 2, and stimulated with insulin for 24 h. NTP mRNA levels were

measured by quantitative real-time RT-PCR. NOS-3 and APP mRNA levels were simultaneously measured. To make comparisons among the three different genes, the results were expressed as mean percentage differences from the corresponding insulin-stimulated controls, which were designated as 100% within each data set (fig. 4). The results showed that NTP mRNA levels were unaffected by treatment with the PD98059 MEKK inhibitor, but significantly reduced by treatment with chemical inhibitors of GSK-3β, p38 MAPK, cyclin-dependent kinase 5 (CDK-5) and protein kinase A (fig. 4A). Western blot analysis with digital image quantification demonstrated similar effects of each kinase inhibitor on the relative changes in NTP protein expression (fig. 4B). Parallel studies demonstrated substantially different effects of the kinase inhibitors on NOS3 and APP mRNA levels in the same insulin-stimulated cells. NOS-3 mRNA expression was increased by treatment with inhibitors of MEKK, p38 MAPK or PKA, and decreased by inhibitors of CDK-5 and GSK-3β (fig. 4C). APP mRNA levels were also strikingly increased by pretreatment with the PKA inhibitor and decreased by pretreatment with the CDK-5 or GSK-3β inhibitor (fig. 4D). Therefore, NTP, APP and NOS-3 share in common the positive regulation of gene expression by GSK-3β signaling.

Insulin modulation of NTP phosphorylation

To demonstrate NTP phosphorylation, cells were metabolically labeled with [^{32}P], and NTP was immunoprecipitated using the cocktail of monoclonal antibodies. Immunoprecipitates were fractionated by SDS-PAGE, transferred to PVDF membranes and detected by autoradiography. [^{32}P]-labeled clusters (~39–60 kD) were observed in both insulin- and IGF-1-stimulated cells. However, pulse-chase metabolic labeling studies demonstrated that phosphorylation of NTP was more prolonged with insulin compared with IGF-1 stimulation (data not shown). Phospho-amino acid analysis using two-dimensional electrophoresis and autoradiography detected phospho-Serine residues in NTP immunoprecipitated

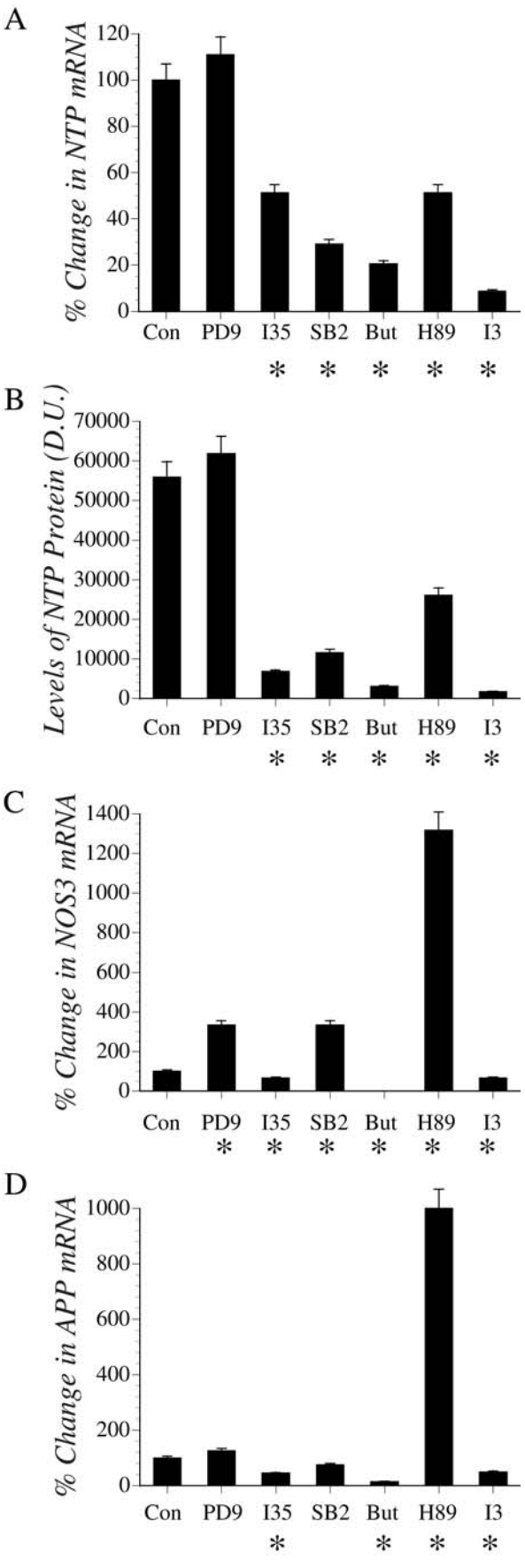

Figure 4. Signaling pathways regulating insulin-stimulated NTP expression: SH-Sy5y cells were pretreated with one of the kinase modulators listed in table 2 and stimulated with insulin for 24 h. (*A*) Cells were analyzed by real-time quantitative RT-PCR to examine changes in the levels of NTP mRNA with defined growth factor stimulation. (*B*) NTP protein levels were measured by Western blot analysis with digital image quantification. Values (mean ± S.D.) are posted in arbitrary densitometry units (D.U.). Parallel real-time quantitative RT-PCR studies were use to measure (*C*) NOS3 and (*D*) APP mRNA transcripts in the same samples. Con, insulin only; PD9, PD98059; I35, indirubin-3′-monoxime, 5-iodo; SB2, SB202190; But, butyrolacetone; H89, H89539; I3- Indirubin-3′-monoxime. See table 2 for concentrations used and the specific kinases targeted for inhibition. All cultures were stimulated with 50 nM insulin (* at least $P < 0.01$ relative to the corresponding insulin-stimulated control).

from insulin or IGF-1 stimulated cells (fig. 5A). Correspondingly, phospho-Serine immunoreactivity was detected in NTP immunoprecipitates obtained from cells stimulated with insulin or IGF-1, but not in unstimulated cells or immunoprecipitates generated with a nonrelevant antibody to hepatitis B virus surface antigen (fig. 5B). Western blot analysis of [^{32}P]-labeled NTP immunoprecipitates using a different NTP monoclonal antibody (N2D12) confirmed that phospho-proteins detected were indeed NTP molecules (data not shown). Anti-phospho-Serine Western blot analysis of NTP immunoprecipitates was used to determine the time course of NTP phosphorylation in relation to insulin stimulation. Those studies demonstrated peak levels of phosphorylated NTP after 60 min of insulin stimulation (fig. 5C).

To identify the kinases that may regulate NTP phosphorylation, SH-Sy5y cells were pretreated for 2 h with a single kinase inhibitor (table 2), then stimulated with insulin for 30 min. NTP immunoprecipitates were probed with antibodies to phospho-Serine by Western blot analysis. The levels of immunoreactivity were measured by band-scanning digital image quantification. The studies demonstrated reduced levels of phospho-NTP in cells treated with Indirubin-3′-monoxime, 5-iodo, LiCl (data not shown), butyrolacetone or SB202190, and increased levels of phospho-NTP in cells treated with LY294002 or chelerythrine chloride (figs 5D, E). Further in vitro studies demonstrated that GSK-3 could phosphorylate purified recombinant NTP, whereas Erk MAPK was ineffective in this regard (fig. 5F).

NTP interactions with neuronal cytoskeletal proteins

There are three independent lines of evidence suggesting that NTP may have a functional role in relation to the neuronal cytoskeleton. (i) In situ studies of human brain tissue demonstrated increased levels of NTP colocalized with phospho-*tau*-immunoreactive cytoskeletal AD lesions [2]. (ii) In vitro experiments demonstrated increased levels of phospho-*tau* in neuronal cells transfected with the AD7c-NTP gene [10, 11]. (iii) In the present report, subcellular fractionation studies detected NTP predominantly within the cytoskeletal fraction. Therefore, it was of interest to determine whether NTP could physically associate with microtubule-associated proteins.

Direct Western blot analysis detected the expected ~39–45 kD NTP proteins. However, under nonreducing conditions, we also detected slower migrating proteins (>110 kD) with NTP immunoreactivity (fig. 6A, left). Anti-NTP immunoblotting of NTP immunoprecipitates confirmed the presence of supershifted NTP-immunoreactive proteins (fig. 6A, right). Direct Western blot analysis of SH-Sy5y cell lysates using polyclonal antibodies to *tau* or monoclonal antibodies to MAP-1b demonstrated the expected bands corresponding to these proteins (figs 6B, D). Immunoprecipitation/Western blot analysis demonstrated *tau* and MAP-1b immunoreactivity in NTP immunoprecipitates (figs 6C, E), and NTP immunoreactivity in *tau* (data not shown) and MAP-1b immunoprecipitates (fig. 6F). The proteins detected by Western blot analysis of immunoprecipitates had retarded migration (larger masses) relative to the proteins detected by direct Western blot analysis under nonreducing conditions.

A potential consequence of protein-protein interaction is ubiquitin-mediated degradation of the complex as a mechanism for regulating turnover of the molecules. To assess the potential biological relevance of the NTP interactions with microtubule-associated proteins, ubiquitin immunoreactivity was examined by direct Western blot analysis and Western blot analysis of NTP immunoprecipitates. Those studies revealed the expected broad size range of ubiquitin immunoreactivity in the cell lysates (fig. 6G), as well as abundant ubiquitin immunoreactivity in NTP immunoprecipitates (fig. 6H). Negative control studies demonstrated abundant expression of aspartyl-(asparaginyl) β-hydroxylase (AAH) [23, 24] in SH-Sy5y cells (fig. 6I), and absent AAH immunoreactivity in the NTP immunoprecipitates (fig. 6J).

Discussion

This study characterizes growth factor modulation of NTP expression in SH-Sy5y human neuronal cells. Using antibodies generated against the recombinant protein, AD7c-NTP, we detected ~39–45 kD and ~18–21 kD NTP-immunoreactive proteins in SH-Sy5y cells, rat cerebral cortex and human temporal lobe. These profiles of NTP expression were previously demonstrated in human brain tissue and cerebrospinal fluid, together with the finding of significantly higher levels of NTP immunoreactivity in AD compared with age-matched control samples [1–4, 6, 25]. The readily detectable expression of NTP in a human neuronal cell line provides a useful in vitro model for investigating the regulation and potential function of this gene.

The quantitative real-time RT-PCR and Western blot analysis studies demonstrated that NTP gene expression was robustly increased by insulin stimulation. Although IGF-1 also stimulated NTP expression, it was less effective than insulin, and in NGF-stimulated cells, NTP mRNA was virtually undetectable. These observations provide the first clear evidence that NTP expression is prominently regulated by insulin, and to a lesser degree by IGF-1, and suggest that NTP expression in the brain may be highest in neurons that express abundant levels of insulin and/or IGF-1 receptors. These findings are of further interest because NTP expression is developmentally regulated [13], and insulin and IGF-1 have important roles in neuronal growth, survival and differentiation

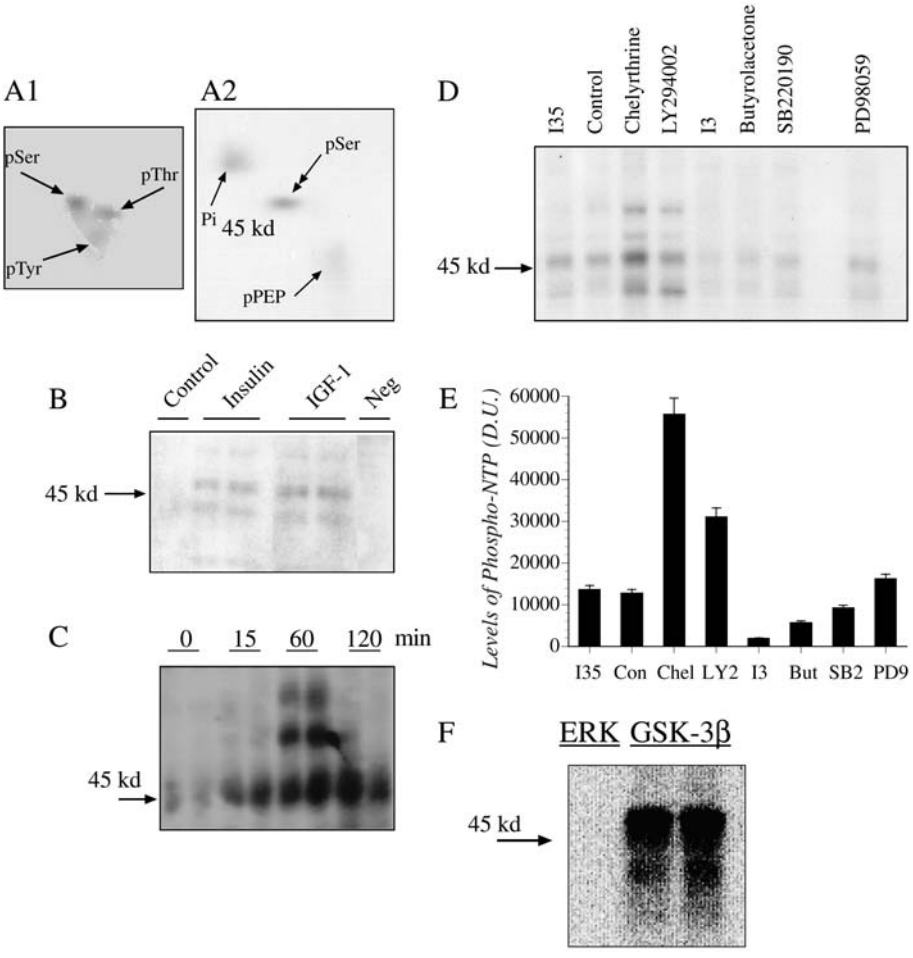

Figure 5. NTP phosphorylation following insulin or IGF-1 stimulation: SH-Sy5y cells were stimulated with 50 nM insulin or 25 nM IGF-1 and metabolically labeled with [^{32}P]-orthophosphate for 2 h, then further incubated for up to 24 h in isotope-free defined medium with continued growth factor stimulation. [^{32}P]-labeled NTP molecules were immunoprecipitated with a cocktail of monoclonal antibodies (N3I4, N2J1, N2U6). The proteins were fractionated by SDS-PAGE, transferred to PVDF membrane and detected by film autoradiography. The positions of NTP proteins (arrowheads) were verified by Western blot analysis of the membrane. (*A*) Phospho-amino acid analysis was used to identify phosphorylated amino acids in NTP. The radiolabeled band corresponding to [^{32}P]-labeled NTP was excised, and the eluted proteins were subjected to acid hydrolysis followed by two-dimensional electrophoresis and autoradiography (see 'Methods'). Positive control ninhydrin-stained phospho-Serine (pSer), phospho-Threonine (pThr) and phospho-Tyrosine (pTyr) standards that were comigrated with the samples are shown in *A1*. pSer was the only phospho-amino acid signal detected in NTP (*A2*). Other spots in *A2* correspond to inorganic phosphate (Pi) and phospho-peptides (pPEP). (*B*) Anti-pSer Western blot analysis of NTP immunoprecipitates from unstimulated (control), and insulin- or IGF-1-stimulated SH-Sy5y cells. The negative control lane (Neg) corresponds to results obtained when nonrelevant antibody to hepatitis B virus was used for immunoprecipitation. (*C*) The time course of insulin-stimulated phosphorylation of NTP was assessed by anti-pSer Western blot analysis of NTP immunoprecipitates. (*D*) To determine potential mechanisms by which insulin regulates NTP phosphorylation, cells were pretreated with one of the kinase inhibitors listed in table 2 and then stimulated with insulin for 2 h. Cells were analyzed by anti-pSer Western blot analysis of NTP immunoprecipitates. (*E*) The phospho-NTP Western blot signals (doublet bands just below the 45-kD standard as shown in (*D*) were scanned, and the densities were quantified using the Kodak Digital Science Image Station. The graph depicts the relative levels of phospho-NTP (densitometry units, D.U.) in cells stimulated with insulin and treated with vehicle, or one of the kinase inhibitors including Indirubin-3′-monoxime, 5-iodo (I35); chelyrithrine chloride (Chel); LY294002 (LY2); Indirubin-3′-monoxime (I3); butyrolacetone (But); SB202190 (SB2) or PD98059 (PD9). See table 2 for concentrations used and the kinase targeted by each inhibitor (*$P < 0.01$ relative to the insulin-stimulated control). (*F*) In vitro phosphorylation of recombinant NTP. Reactions were performed in the presence of [γ^{32}P]ATP, recombinant NTP protein, and activated Erk MAPK or GSK-3β. NTP immunoprecipitates were fractionated by SDS-PAGE, and the radiolabeled products were detected by autoradiography. In *B*, *C*, *D*, and *F*, the positions of molecular weight standards are shown at the left with arrows.

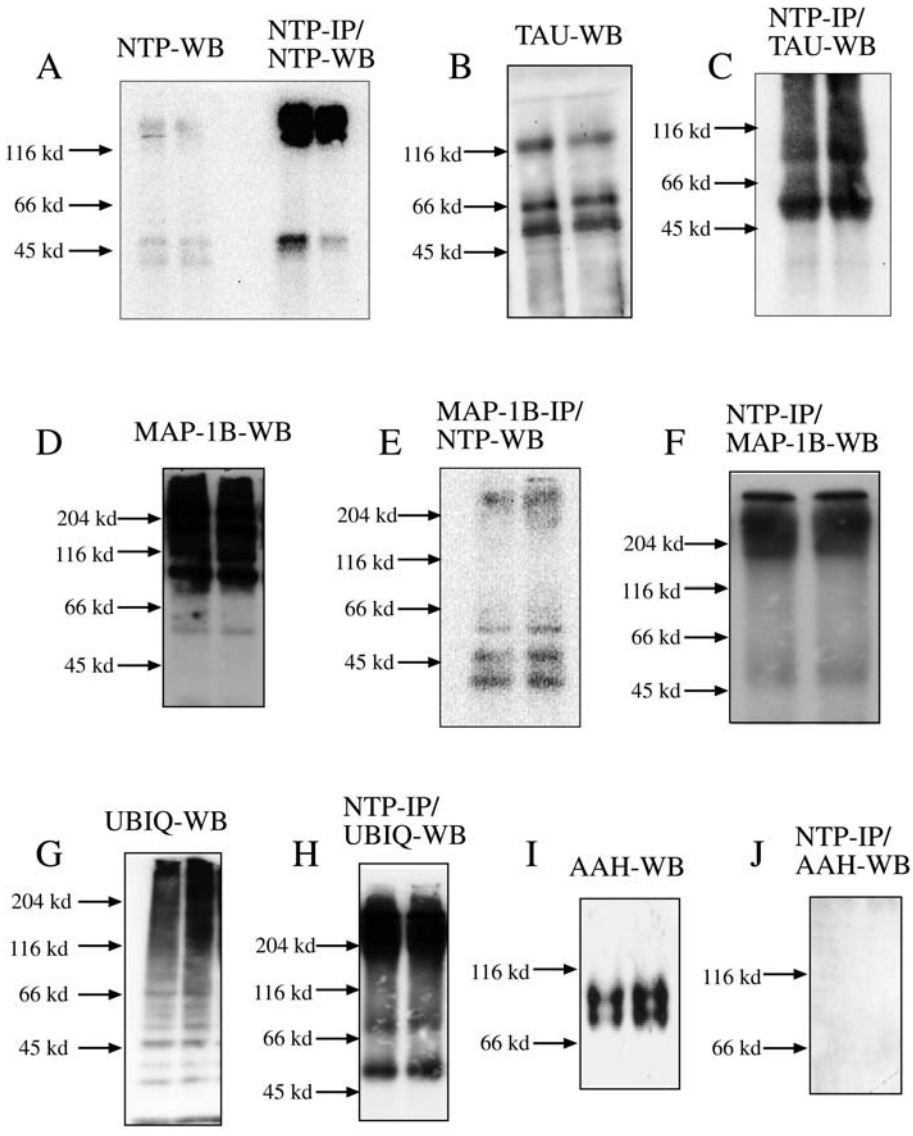

Figure 6. Coimmunoprecipitation of NTP with neuronal microtubule-associated proteins and ubiquitin. (*A*) Direct Western blot analysis (NTP-WB), and Western blot analysis of NTP immunoprecipitates (NTP-IP/NTP-WB) using antibodies to NTP. (*B*) Western blot analysis detection of *tau* expression in SH-Sy5y cells. (*C*) *Tau* immunoreactivity in NTP immunoprecipitates. (*D*) MAP-1b expression in SH-Sy5y cells. (*E*) NTP immunoreactivity in MAP-1b immunoprecipitates. (*F*) MAP-1b immunoreactivity in NTP immunoprecipitates. (*G*) Ubiquitin immunoreactivity in SH-Sy5y cells. (*H*) Ubiquitin immunoreactivity in NTP immunoprecipitates. As a negative control, (*I*) Western blot analysis was used to detect aspartyl-(asparaginyl)-β-hydroxylase (AAH) in SH-Sy5y cells and (*J*) demonstrate the absence of AAH immunoreactivity in NTP immunoprecipitates. The positions of molecular weigh standards are shown at the left of each panel.

[26–29]. Moreover, emerging evidence suggests that some aspects of AD-associated pathology may be linked to alterations in insulin signaling or function in the brain [26, 29, 30]. Although *tau* protein levels were also modulated by growth factor stimulation, in contrast to NTP, IGF-1 and NGF were more effective than insulin. The selectivity of the observed growth factor-stimulated responses was further demonstrated by the modest or absent modulation of NOS-3, APP and Erk MAPK expression in the insulin- and IGF-1-stimulated cells. Together, these results suggest that NTP expression is regulated somewhat differently from molecules such as *tau*, APP and NOS-3, which are also implicated in the pathobiology of AD [20, 21, 31–34]. The differential effects of insulin compared with NGF were not due to poor cellular responses to NGF since *tau* protein was robustly upregulated by NGF stimulation.

To characterize the signaling pathways that mediate insulin-stimulated NTP expression, the cells were pretreated with kinase inhibitors, and insulin-stimulated NTP expression was measured using quantitative real-time RT-PCR and Western blot analysis. The results showed that NTP mRNA and protein levels were significantly reduced in cells that were treated with inhibitors of

p38 MAPK, Cdk-5, GSK-3β or PKA. However, the GSK-3β inhibitors were most effective and nearly abolished NTP expression, suggesting that GSK-3β activity promotes NTP expression. Although high levels of GSK-3β activity promote apoptosis [35, 36], physiological levels of GSK-3β inhibit growth and proliferation mechanisms [37–39], and promote cytoskeletal assembly [40–44]. Since activation of p38 MAPK [45] or overexpression of cdk-5 [46] can result in increased levels of GSK-3β activity, the observed moderate inhibition of NTP following inhibition of those kinases may have been due to indirect inhibition of GSK-3β. On the other hand, the reduced levels of NTP observed in cells treated with the PKA inhibitor may have been mediated by a different mechanism or pathway, since PKA typically inhibits GSK-3β by phosphorylating Akt kinase [47, 48] and therefore a PKA inhibitor would be expected to increase GSK-3β activity. Similarly, p38 MAPK and Cdk-5 may also function through GSK-3β-independent mechanisms to upregulate NTP expression.

Additional studies showed that the levels of both NOS-3 and APP mRNA were prominently increased in cells treated with a PKA inhibitor and reduced in cells treated with an inhibitor of GSK-3β, Cdk-5 or p38 MAPK. These results suggest that the NTP, NOS-3 and APP genes are transcriptionally modulated by similar mechanisms in insulin-stimulated neuronal cells. In this regard, GSK-3β seems to have a pivotal role. On the other hand, the finding that insulin signaling through PKA stimulates NTP but inhibits NOS-3 and APP provides evidence for distinct mechanisms by which these genes are regulated. The implication of these findings is that in AD, abnormalities in the expression or function of genes that have been linked to neurodegeneration may arise through complex mechanisms, some of which may be shared and others distinct.

The studies showed that NTP was phosphorylated on Serine residues following insulin or IGF-1 stimulation. The kinase inhibitor studies demonstrated reduced levels of phosphorylated NTP in cells treated with inhibitors of GSK-3β, and increased levels of phospho-NTP in cells treated with LY294002, which inhibits phosphatidylinositol-3-kinase (PI3) kinase, or chelerythrine chloride, which inhibits PKC. Since inhibition of PI3 kinase [49] or PKC [50–52] could result in increased levels of GSK-3β activity, additional in vitro kinase studies were used to demonstrate that recombinant NTP could be phosphorylated by GSK-3β. These results correspond well with the computer-assisted subsequence analysis which predicted the presence of 14 GSK-3β phosphorylation sites on NTP [1], and are of particular interest because GSK-3β also phosphorylates *tau* [43, 53] and MAP-1b [40, 41], which accumulate in degenerating AD brain neurons.

Insulin- and IGF-1-stimulated signaling through PI3 kinase and Akt typically lead to inhibition of GSK-3β activity. However, this effect generally occurs within 10 or 15 min of adding the growth factors, and subsequently, as Akt activity subsides, GSK-3β activity resurges [54]. In our experiments, peak levels of NTP phosphorylation were observed 60 min after adding insulin or IGF-1 to the culture medium. Therefore, the observed phosphorylation of NTP could not have represented a direct effect of insulin or IGF-1 stimulation, and instead probably corresponded to the poststimulatory state in which PI3 kinase and Akt were no longer activated and GSK-3 was disinhibited.

Phospho-*tau*-immunoreactive neuronal cytoskeletal lesions represent one of the characteristic CNS abnormalities that correlate with dementia in AD [55–58]. The colocalization of AD7c-NTP immunoreactivity with phospho-*tau* in brains with AD [2], and the finding that phospho-*tau* and NTP increase coincidentally early in the course of AD [6] suggested a link between these two molecules in relation to AD-type neurodegeneration. We performed studies to investigate potential physical interactions between NTP and *tau* or MAP-1b. The studies showed that NTP proteins were abundantly distributed in the cytoskeletal fraction, and that both *tau* and MAP-1b were coimmunoprecipitated with NTP. Therefore, NTP has a subcellular localization that permits its physical association with neuronal microtubule-associated proteins. Although the functional significance of NTP-*tau* and NTP-MAP-1b complexes has not yet been determined, further studies demonstrating increased ubiquitin immunoreactivity in the NTP immune complexes suggest a role for NTP in the processing, degradation or turnover of neuronal cytoskeletal proteins, as would be required for growth, neuritic sprouting and synaptic plasticity. Aberrant neuritic sprouting with increased levels of cytoskeletal and growth-associated proteins represents another characteristic dementia-associated abnormality in AD [59–62].

Acknowledgment. Supported by grants AA12458, AA02666 and AA11931 from the National Institute of Alcoholism and Alcohol Abuse, and COBRE Award P20RR15578 from the National Institutes of Health.

1 de la Monte S. M., Ghanbari K., Frey W. H., Beheshti I., Averback P., Hauser S. L. et al. (1997) Characterization of the AD7c-NTP cDNA expression in Alzheimer's disease and measurement of the 41-kD protein in cerebrospinal fluid. J. Clin. Invest. **100:** 1–12

2 de la Monte S. M., Carlson R. I., Brown N. V. and Wands J. R. (1996) Profiles of neuronal thread protein expression in Alzheimer's disease. J. Neuropathol. Exp. Neurol. **55:** 1038–1050

3 de la Monte S. M., Ghanbari H., Ghanbari K., Averbach P. and Wands J. R. (1999) AD7c-NTP biomarker for Alzheimer's disease. Alz Reports **2:** 327–332

4 Ghanbari H., Ghanbari K., Munzar M. and Averback P. (1998) Specificity of AD7c-NTP as a biochemical marker for Alzheimer's disease. J. Contemp. Neurol. **2:** 2–6

5 Ghanbari H., Ghanbari K., Beheshti I., Munzar M., Vasauskas A. and Averback P. (1998) Biochemical assay for AD7C-NTP

in urine as an Alzheimer's disease marker. J. Clin. Lab. Anal. **12:** 285–288
6 Kahle P. J., Jakowec M., Teipel S. J., Hampel H., Petzinger G. M., Di Monte D. A. et al. (2000) Combined assessment of tau and neuronal thread protein in Alzheimer's disease CSF. Neurology **54:** 1498–1504
7 de la Monte S. M., Volicer L., Hauser S. L. and Wands J. R. (1992) Increased levels of neuronal thread protein in cerebrospinal fluid of patients with Alzheimer's disease. Ann. Neurol. **32:** 733–742
8 de la Monte S. M. and Wands J. R. (1992) Neuronal thread protein over-expression in brains with Alzheimer's disease lesions. J. Neurol. Sci. **113:** 152–164
9 Ozturk M., de la Monte S. M., Gross J. and Wands J. R. (1989) Elevated levels of an exocrine pancreatic secretory protein in Alzheimer disease brain. Proc. Natl. Acad. Sci. USA **86:** 419–423
10 de la Monte S. M. and Wands J. R. (2001) Alzheimer-associated neuronal thread protein induced apoptosis and impaired mitochondrial function in human central nervous system-derived neuronal cells. J. Neuropathol. Exp. Neurol. **60:** 195–207
11 de la Monte S. M. and Wands J. R. (2001) Neurodegeneration changes in primary central nervous system neurons transfected with the Alzheimer-associated neuronal thread protein gene. Cell. Mol. Life Sci. **58:** 844–849
12 de la Monte S. M. and Wands J. R. (2002) The AD7c-ntp neuronal thread protein biomarker for detecting Alzheimer's disease. Front. Biosci. **7:** d989–996
13 de la Monte S. M., Xu Y. Y., Hutchins G. M. and Wands J. R. (1996) Developmental patterns of neuronal thread protein gene expression in Down syndrome. J. Neurol. Sci. **135:** 118–125
14 de la Monte S. M., Garner W. and Wands J. R. (1997) Neuronal thread protein gene modulation with cerebral infarction. J. Cereb. Blood Flow Metab. **17:** 623–635
15 de la Monte S. M., Xu Y. Y. and Wands J. R. (1996) Modulation of neuronal thread protein expression with neuritic sprouting: relevance to Alzheimer's disease. J. Neurol. Sci. **138:** 26–35
16 Xu Y. Y., Bhavani K., Wands J. R. and de la Monte S. M. (1995) Ethanol inhibits insulin receptor substrate-1 tyrosine phosphorylation and insulin-stimulated neuronal thread protein gene expression. Biochem. J. 125–132
17 Xu Y. Y., Bhavani K., Wands J. R. and de la Monte S. M. (1995) Insulin-induced differentiation and modulation of neuronal thread protein expression in primitive neuroectodermal tumor cells is linked to phosphorylation of insulin receptor substrate-1. J. Mol. Neurosci. **6:** 91–108
18 Imahori K. and Uchida T. (1997) Physiology and pathology of tau protein kinases in relation to Alzheimer's disease. J. Biochem. **121:** 179–188
19 de la Monte S. M., Chiche J., von dem Bussche A., Sanyal S., Lahousse S. A., Janssens S. P. et al. (2003) Nitric oxide synthase-3 overexpression causes apoptosis and impairs neuronal mitochondrial function: relevance to Alzheimer's-type neurodegeneration. Lab. Invest. **83:** 287–298
20 Sohn Y. K., Ganju N., Bloch K. D., Wands J. R. and de la Monte S. M. (1999) Neuritic sprouting with aberrant expression of the nitric oxide synthase III gene in neurodegenerative diseases. J. Neurol. Sci. **162:** 133–151
21 de la Monte S. M., Lu B., Sohn Y., Etienne D., Kraft J., Ganju N. et al. (2000) Aberrant expression of nitric oxide synthase III in Alzheimer's disease: relevance to cerebral vasculopathy and neurodegeneration. Neurobiol. Aging **21:** 309–319
22 Ausubel F. M., Brent R., Kingston R. E., Moore D. D., Seidman J. G., Smith J. A. et al. (2002) Current Protocols in Molecular Biology, Wiley, New York
23 Sepe P. S., Lahousse S. A., Gemelli B., Chang H., Maeda T., Wands J. R. et al. (2002) Antisense inhibition of aspartyl (asparaginyl)-beta hydroxylase mediated neuroblastoma cell migration. Lab. Invest. **82:** 881–891
24 Lavaissiere L., Jia S., Nishiyama M., de la Monte S., Stern A. M., Wands J. R. et al. (1996) Overexpression of human aspartyl(asparaginyl)beta-hydroxylase in hepatocellular carcinoma and cholangiocarcinoma. J. Clin. Invest. **98:** 1313–1323
25 Fitzpatrick J., Munzar M., Fochi M., Bibiano R. and Averback P. (2000) 7c Gold urinary assay of neural thread protein in Alzheimer's disease. Alz. Reports **3:** 155–159
26 Zhao W. and Alkon D. L. (2001) Role of insulin and insulin receptor in learning and memory. Mol. Cell. Endocrinol. **177:** 125–134
27 Joshi R. L., Lamothe B., Cordonnier N., Mesbah K., Monthioux E., Jami J. et al. (1996) Targeted disruption of the insulin receptor gene in the mouse results in neonatal lethality. EMBO J. **15:** 1542–1547
28 Bruning J. C., Gautam D., Burks D. J., Gillette J., Schubert M., Orban P. C. et al. (2000) Role of brain insulin receptor in control of body weight and reproduction. Science **289:** 2122–2125
29 Freychet P. (2000) Insulin receptors and insulin actions in the nervous system. Diabetes Metab. Res. Rev. **16:** 390–392
30 Hoyer S. and Lannert H. (1999) Inhibition of the neuronal insulin receptor causes Alzheimer-like disturbances in oxidative/energy brain metabolism and in behavior in adult rats. Ann. N. Y. Acad. Sci. **893:** 301–303
31 Beyreuther K., Bush A. I., Dyrks T., Hilbich C., Konig G., Monning U. et al. (1991) Mechanisms of amyloid deposition in Alzheimer's disease. Ann. N. Y. Acad. Sci. **640:** 129–139
32 Behl C. and Sagara Y. (1997) Mechanism of amyloid beta protein induced neuronal cell death: current concepts and future perspectives. J. Neural. Transm. Suppl. **49:** 125–134
33 Probst A., Langui D., Ipsen S., Robakis N. and Ulrich J. (1991) Deposition of beta/A4 protein along neuronal plasma membranes in diffuse senile plaques. Acta Neuropathol. **83:** 21–29
34 de la Monte S. M. and Bloch K. D. (1997) Aberrant expression of the constitutive endothelial nitric oxide synthase gene in Alzheimer disease. Mol. Chem. Neuropathol. **30:** 139–159
35 Hetman M., Cavanaugh J. E., Kimelman D. and Xia Z. (2000) Role of glycogen synthase kinase-3beta in neuronal apoptosis induced by trophic withdrawal. J. Neurosci. **20:** 2567–2574
36 Eves E. M., Xiong W., Bellacosa A., Kennedy S. G., Tsichlis P. N., Rosner M. R. et al. (1998) Akt, a target of phosphatidylinositol 3-kinase, inhibits apoptosis in a differentiating neuronal cell line. Mol. Cell. Biol. **18:** 2143–2152
37 Rossig L., Badorff C., Holzmann Y., Zeiher A. M. and Dimmeler S. (2002) Glycogen synthase kinase-3 couples AKT-dependent signaling to the regulation of p21Cip1 degradation. J. Biol. Chem. **277:** 9684–9689
38 Hardt S. E. and Sadoshima J. (2002) Glycogen synthase kinase-3beta: a novel regulator of cardiac hypertrophy and development. Circ. Res. **90:** 1055–1063
39 Kim H. S., Skurk C., Thomas S. R., Bialik A., Suhara T., Kureishi Y. et al. (2002) Regulation of angiogenesis by glycogen synthase kinase-3beta. J. Biol. Chem. **277:** 41888–41896
40 Lucas F. R., Goold R. G., Gordon-Weeks P. R. and Salinas,P. C. (1998) Inhibition of GSK-3beta leading to the loss of phosphorylated MAP-1B is an early event in axonal remodelling induced by WNT-7a or lithium. J. Cell. Sci. **111 (Pt 10):** 1351–1361
41 Salinas P. C. (1999) Wnt factors in axonal remodelling and synaptogenesis. Biochem. Soc. Symp. **65:** 101–109
42 Krylova O., Messenger M. J. and Salinas P. C. (2000) Dishevelled-1 regulates microtubule stability: a new function mediated by glycogen synthase kinase-3beta. J. Cell. Biol. **151:** 83– 94
43 Sang H., Lu Z., Li,Y., Ru B., Wang W. and Chen J. (2001) Phosphorylation of tau by glycogen synthase kinase 3beta in intact mammalian cells influences the stability of microtubules. Neurosci. Lett. **312:** 141–144
44 Sayas C. L., Avila J. and Wandosell F. (2002) Regulation of neuronal cytoskeleton by lysophosphatidic acid: role of GSK-3. Biochim. Biophys. Acta **1582:** 144–153

45 Blair A. S., Hajduch E., Litherland G. J. and Hundal H. S. (1999) Regulation of glucose transport and glycogen synthesis in L6 muscle cells during oxidative stress. Evidence for cross-talk between the insulin and SAPK2/p38 mitogen-activated protein kinase signaling pathways. J. Biol. Chem. **274:** 36293–36299
46 Noble W., Olm V., Takata K., Casey E., Mary O., Meyerson J. et al. (2003) Cdk5 is a key factor in tau aggregation and tangle formation in vivo. Neuron **38:** 555–565
47 Filippa N., Sable C. L., Filloux C., Hemmings B. and Van Obberghen E. (1999) Mechanism of protein kinase B activation by cyclic AMP-dependent protein kinase. Mol. Cell. Biol. **19:** 4989–5000
48 Li M., Wang X., Meintzer M. K., Laessig T., Birnbaum M. J. and Heidenreich K. A. (2000) Cyclic AMP promotes neuronal survival by phosphorylation of glycogen synthase kinase 3beta. Mol. Cell. Biol. **20:** 9356–9363
49 Pap M. and Cooper G. M. (1998) Role of glycogen synthase kinase-3 in the phosphatidylinositol 3-Kinase/Akt cell survival pathway. J. Biol. Chem. **273:** 19929–19932
50 Doornbos R. P., Theelen M., van der Hoeven P. C., van Blitterswijk W. J., Verkleij A. J. and van Bergen en Henegouwen P. M. (1999) Protein kinase Czeta is a negative regulator of protein kinase B activity. J. Biol. Chem. **274:** 8589–8596
51 Standaert M. L., Bandyopadhyay G., Antwi E. K. and Farese R. V. (1999) RO 31-8220 activates c-Jun N-terminal kinase and glycogen synthase in rat adipocytes and L6 myotubes. Comparison to actions of insulin. Endocrinology **140:** 2145–2151
52 Tsujio I., Tanaka T., Kudo T., Nishikawa T., Shinozaki K., Grundke-Iqbal I. et al. (2000) Inactivation of glycogen synthase kinase-3 by protein kinase C delta: implications for regulation of tau phosphorylation. FEBS Lett. **469:** 111–117
53 Lovestone S., Reynolds C. H., Latimer D., Davis D. R., Anderton B. H., Gallo J. M. et al. (1994) Alzheimer's disease-like phosphorylation of the microtubule-associated protein tau by glycogen synthase kinase-3 in transfected mammalian cells. Curr. Biol. **4:** 1077–1086
54 de la Monte S. M. and Wands J. R. (2002) Chronic gestational exposure to ethanol impairs insulin-stimulated survival and mitochondrial function in cerebellar neurons. Cell. Mol. Life Sci. **59:** 882–893
55 Joachim C. L., Morris J. H., Selkoe D. J. and Kosik K. S. (1987) Tau epitopes are incorporated into a range of lesions in Alzheimer's disease. J. Neuropathol. Exp. Neurol. **46:** 611–622
56 Kosik K. S., Joachim C. L. and Selkoe D. J. (1986) Microtubule-associated protein tau (tau) is a major antigenic component of paired helical filaments in Alzheimer disease. Proc. Natl. Acad. Sci. USA **83:** 4044–4048
57 McKee A. C., Kosik K. S. and Kowall N. W. (1991) Neuritic pathology and dementia in Alzheimer's disease. Ann. Neurol. **30:** 156–165
58 Schmidt M. L., Lee V. M. and Trojanowski J. Q. (1990) Relative abundance of tau and neurofilament epitopes in hippocampal neurofibrillary tangles. Am. J. Pathol. **136:** 1069–1075
59 de la Monte S. M., Ng S. C. and Hsu D. W. (1995) Aberrant GAP-43 gene expression in Alzheimer's disease. Am. J. Pathol. **147:** 934–946
60 Ihara Y. (1988) Massive somatodendritic sprouting of cortical neurons in Alzheimer's disease. Brain Res. **459:** 138–144
61 Scheibel A. B. and Tomiyasu U. (1978) Dendritic sprouting in Alzheimer's presenile dementia. Exp. Neurol. **60:** 1–8
62 Masliah E., Mallory M., Hansen L., Alford M., Albright T., DeTeresa R. et al. (1991) Patterns of aberrant sprouting in Alzheimer's disease. Neuron **6:** 729–739